TweetS@: A 3D Printed Tweeting CubeSat with a Neural Network Sun Sensor

Yiwei Mao[1], Jack Liell-Cock[1], Sholto Douglas[1], Stephen Huang[1], Qian Cheng[1], Ryan Jeffreson[1], Jamie De Piero[1], Shaka Chu[1], Tom McCredie[1], and Muddasir Tahir[1]

The University of Sydney, NSW, 2006, Australia

Summary. The goal of TweetS@ (pronounced Tweet-Sat) is to foster public interest and awareness of space engineering by enabling direct interaction through Twitter. TweetS@ is a 3D printed two-unit CubeSat designed with ease of assembly in mind and is tasked with fulfilling tweet requests for image captures. The structure was verified through structural and thermal simulations and a rocket launch to 10,000 ft. We also present SolarNet, a novel sun vector predictor using a neural network that uses solar panel current and photodiode readings.

Keywords: CubeSats, Twitter, 3D Printing, Neural Network, Sun Sensor

Introduction

Funding provided to scientific research and development is strongly correlated to community interest and involvement. Without the ability to broadcast Neil Armstrong's first steps on the lunar surface to televisions around the world, the 1969 Moon landing would not have achieved its significant cultural impact. The ability to witness rocket launches and other scientific events first-hand drew huge community interest, helping justify funding of the space program for decades. Today, social media is the primary driver of community interaction and engagement with the ability to record, upload and communicate thoughts, ideas and experiments across the world almost instantly.

This paper details the design and successful testing of a modular, low cost 2U CubeSat devised to exploit social media to fuel greater interest in space engineering. Our three main objectives were:

1. Demonstrate tweet functionality on the ground.
2. Prove a 3D printed structure that is capable of surviving launch conditions and a space environment.
3. Validate the performance of SolarNet, a neural network for predicting the sun vector from solar panel current and photodiode measurements.

Twitter Operation

Twitter is a social media platform that allows users to 'tweet' messages up to 140 characters long to their followers. The simplicity of the platform enables information and advertising to be distributed to 330 million active users who send over 500 million tweets per day [1]. For this reason, major space organisations such as NASA, ESA, JAXA, and SpaceX use Twitter to promote their activities. We took this connectivity one step further, letting users interact directly with TweetS@. This allowed a wide and varying audience to explore the exciting world of space engineering and the capabilities of the Australian space industry. TweetS@'s interactivity could engage the emerging social media focused generation and encourage ideas of space exploration.

Twitter Bot Software

As part of the mission, a ground-based software package was developed to allow the public to interact with TweetS@. A user could tweet their desired coordinates to TweetS@'s Twitter handle[1]. Then, an image of the location was captured during the satellite's next pass and downlinked to reply to the original tweet.

The Twitter bot software was developed in Python 3.7 and used the tweepy package[2] to obtain an OAuth-authenticated Twitter application program interface (API) wrapper, which was used to interact with the Twitter network. The software performed three functions:

i. Identification of imaging requests sent through Twitter.
ii. Sorting of requests and generation of uplink data packets.
iii. Reception and relay of satellite imagery to Twitter users.

The Twitter API wrapper's timeline methods were used to scan incoming tweets for imaging requests in the form of geodetic coordinates, or the names of major cities. API information was also used to identify and timestamp requests, so that they could be effectively sorted and addressed when satellite imagery was received. A strong emphasis was placed on versatility for Twitter users, and therefore many input formats were allowed with common mistakes accounted for to ensure a streamline user experience. All successful requests were stored for sorting and if no request was identified within a tweet, the user was prompted for clarification.

After the coordinate requests were identified, a priority queue of all pending requests was created. This determined which requests were sent to the satellite when it next passed the ground station. Revisit times of a given location were up to a week, so the wait time of all users was minimised by imaging locations the satellite was about to pass first. An orbit simulation class was developed to perform revisit time analysis, which returned TweetS@'s position over the next three orbits. A sorting class was created to generate a priority queue based on the output of the simulation instance. The location of each pending request (within a visibility mask defined by TweetS@'s optics and pointing capability) was searched for in the simulation output. If a location was predicted to be visible to TweetS@, the time of passage was recorded.

Rather than providing a set of coordinates, it was easier to send the satellite a set of times when images were to be taken, which was compared to the onboard GPS time. Therefore, the only imaging information that was sent in the uplink packets was the number of seconds since J2000 for each requested image location. Downlinked data packets contained the requested image and its capture time with respect to J2000 (which was used to associate the image to the request tweet). The API ID of the tweet was used to reply to the Twitter user with the satellite imagery.

Payload Results

During testing, TweetS@ was able to successfully downlink and tweet several images to its Twitter account following tweet requests. The image was reduced to a resolution of 320×240 pixels to minimise the downlink time to the ground station. A tweet of the image with the tagged Twitter account was then generated in response to the original request.

The image quality was sufficient to capture the general details of a scene, as shown from the successful test image capture and reply tweet[3] of our team in Figure 1. However, with more efficient compression and higher communication bandwidth, the image quality could be increased.

[1] Twitter handle is @ripwarwick

[2] http://docs.tweepy.org/en/v3.8.0/api.html

[3] https://twitter.com/ripwarwick/status/1136486410947518464

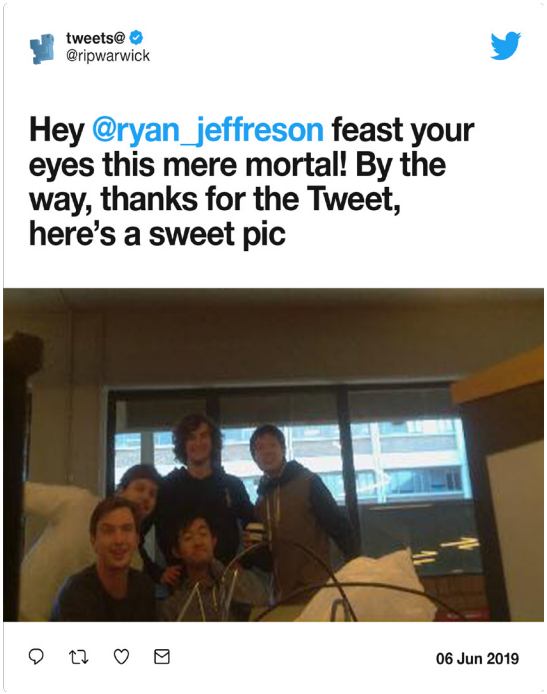

Fig.1: Successful image and tweet from TweetS@.

Radio Communication in Orbit

To communicate with TweetS@, we used the RFD 900+ Modem[4] which had a transmit power of +30 dBm (0 dbW) at 1 W with a RFDFLEX1 900 MHz Flexible PCB Antenna (300 mm RPSMA) as this could be pre-installed and would not have to be deployed once the spacecraft itself was deployed. The operation frequency was set to 915–928 MHz, just above the commonly used '33 cm Wavelength Band' of the UHF spectrum. For our ground station transceiver, we targeted a Yagi antenna with a 16 dBi gain and a transmit power of 17 dBi. Fashioned after the data structure of an Ethernet frame [2], TweetS@ transmits engineering (status) and science (images) packets and accepts command packets; beginning with a header and ending with a checksum for error detection.

In order to obtain images with consistent solar radiance, a Low Earth Orbit (LEO) sun synchronous orbit was planned for TweetS@. The high inclination angle would allow TweetS@ to sight the Troll research station (72.0114°S, 2.5350°E) an average of 10 times a day with a visibility window of 63 minutes. With a bitrate of 64 kb/s, a 1920×1080 RGB image would take 10 minutes to transmit without compression. To service more users, the software can downsize images. All considered, TweetS@'s theoretical downlink and uplink margin was 6.1 dB and 33.5 dB respectively. We were only able to test the radio connection within a confined lab, but our link budget indicated that TweetS@ would be able to communicate in orbit.

3D Printed Structure

A traditional aluminium based chassis was initially proposed due to its strength to weight ratio and its proven use in many CubeSat applications. However, due to the limited machining capabilities available, we opted to use an ABS plastic printed chassis. 3D printed ABS plastic is weaker and lighter than aluminium, so the chassis was made thicker in sections to maintain

[4] http://store.rfdesign.com.au/rfd-900p-modem/

structural integrity and a comparable weight. After preliminary modelling, the reduction of usable volume was found to be 5 mm in all directions - which was not an issue with packaging. ABS plastic was also used to manufacture most custom component mounts.

The significant advantage of 3D printing was its quick manufacturing time (8–10 hour print time), as opposed to the aforementioned week based aluminium option. This allowed for prototyping and quick design changes when necessary and provided the flexibility to deal with unexpected developments. According to Candini et al., ABS is a suitable material for a LEO environment, capable of surviving radiation and heat from solar albedo. Candini et al. found that ABS was resistant to sudden temperature changes in a thermal shock test that cycled between -20 ◦C and 60 ◦C [3].

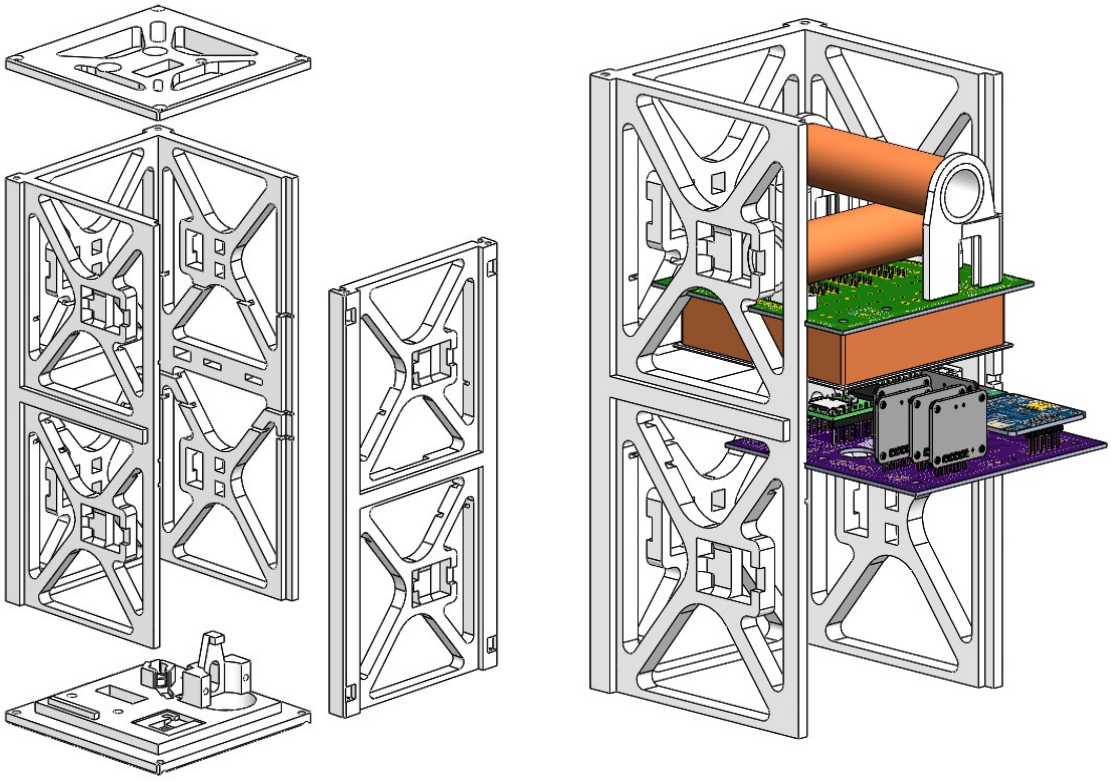

(a) Exploded View of TweetS@ 3D Printed Structure

(b) PCB Assemblies being able to slide in and out along the housing slots

Fig.2: The 3D printed TweetS@ structure and how components fit together.

Ease of Assembly

Due to the small-scale nature of this project, the chassis design focused on ease of assembly and modularisation of components to facilitate repairs and component changes. The chassis shown in Figure 2a comprised of four main sections: the main housing, the top and bottom end caps, and side housing.

Slots were incorporated into the housings shown in Figure 2b for the printed circuit board (PCB) assemblies so partitions holding components such as the battery and transceiver could be slid in and out. After testing the fit with a prototype, it was found that a transition fit was achieved from the Upbox 3D printers and there were no issues with the printer's precision. This meant no boards were loose and thus, no additional securing was required.

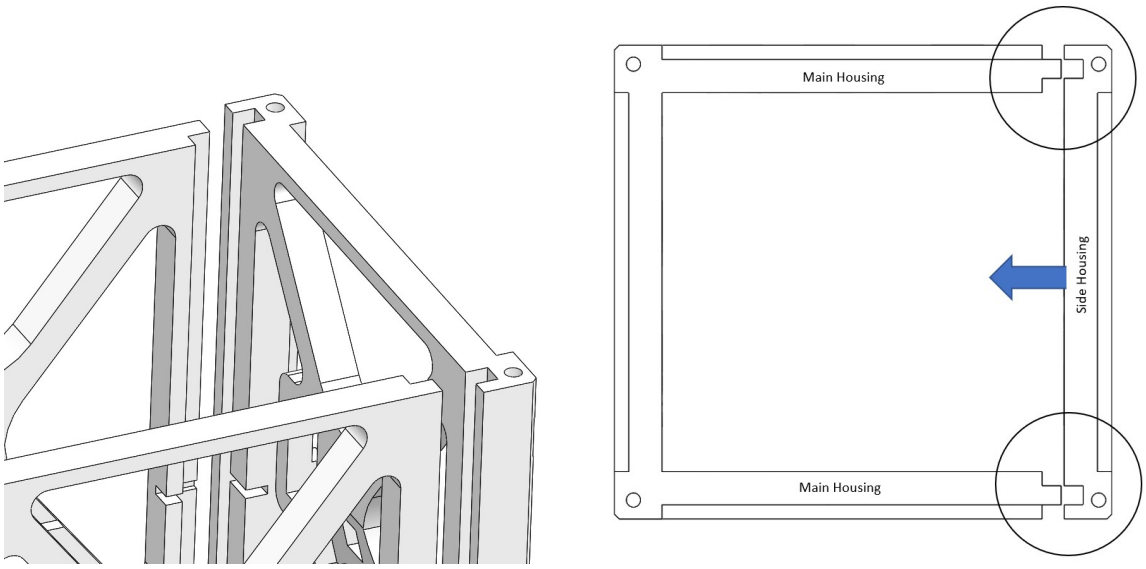

(a) Locking Rail Isometric View

(b) Locking Rail Top View

Fig.3: Satellite Locking Rail Mechanism

A rail locking mechanism was incorporated into the main and side housings allowing ease of assembly, as shown in Figure 3. The entire structure was secured using eight M3×20 countersunk bolts and corresponding captive nuts at the 8 corners of the spacecraft. Having the nuts reside in part of the structure (shown in Figure 4), not only maximised available space, but removed the need of a spanner to hold the nut when fastening the bolt. The recess in which the nut resided was hexagonal in shape, preventing the nuts from turning.

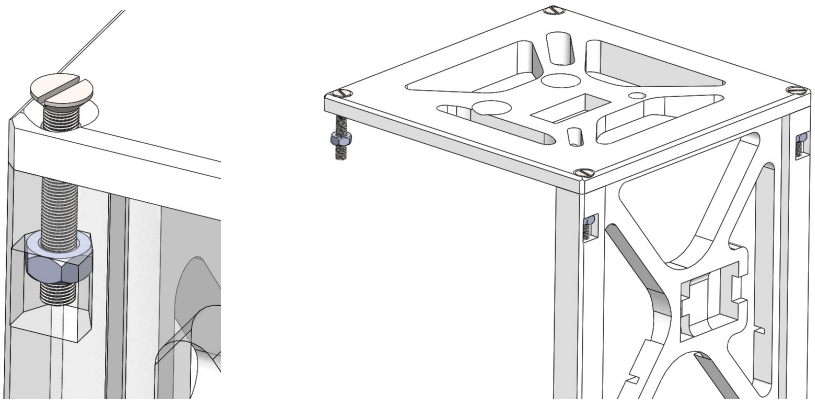

(a) Nut & Bolt securing an end cap to a housing - Close Up

(b) Nut & Bolt securing Top Cap to Side Housing (Main Housing has been removed for clarity)

Fig.4: Captive Nut Details

Vibration Results and Analysis

Finite element method (FEM) simulations and physical tests for quasi-static, resonance, sinusoidal and random vibration cases were required to meet the requirements listed in Table 1.

Test	Requirement
Quasi-Static and G-loads	13 g acceleration
Resonance	Fundamental frequency > 90 Hz 5–100 Hz: 0.15 g
Sinusoidal Vibration	5–100 Hz: 2.5 g 100–125 Hz: 1.25 g
Random Vibration	20 Hz: 0.01125 g^2/Hz 130 Hz: 0.05625 g^2/Hz 800 Hz: 0.05625 g^2/Hz 2000 Hz: 0.015 g^2/Hz
Shock Load	Two shocks along each of the 3 axes 100 Hz: 30 g, 1000 Hz: 700 g, 2000 Hz: 700 g, 5000 Hz: 400 g

Table 1: Various tests and their requirements including the frequencies and amplitude of the input loads where g is Earth's gravitational acceleration and g^2/Hz is the power spectral density function for acceleration.

Natural Frequency						
Mode	**1**	**2**	**3**	**4**	**5**	**6**
Frequencies (Hz)	353.93	365.91	450.24	459.09	556.95	744.73

Table 2: The obtained natural frequencies using FEM.

Table 2 shows the first six eigenmodes of the structure while Table 3 shows the maximum stress concentration within the structure for each test case. The first mode of vibration for the structure was approximately 350 Hz which was well above the required 90 Hz limit specified in Table 1. ABS plastic has a tensile stress of approximately 40 MPa [3], and when printed with 60% infill, our structure passed all tests as shown in Table 3. The maximum stress occurred during the shock load test.

Maximum Equivalent Stress (MPa)			
	Qualification	**Acceptance**	**Protoflight**
Quasi-Static and G-loads	2.5	Not Required	2.08
Sinusoidal Vibration	0.266	0.213	0.266
Random Vibration	1.826	15.841	1.826
Shock Load Test	176.65	Not Required	51.233

Table 3: The obtained maximum equivalent stress of the test cases using FEM.

A loading of 200 m/s^2 was used for all shock load frequencies since the rocket launch was expected to have a maximum of 100 m/s^2, and we designed for a factor of safety of 2. Figure 5 shows the location of the maximum stress concentration of the shock load qualification test. The maximum stress concentration occurred at the legs of the magnetorquer and the bottom plate screw hole. Here, the magnitude of stress was approximately 5 MPa which was well below the ultimate tensile strength of ABS plastic [3]. We therefore concluded that the satellite could survive the shock load experienced during a launch. In fact, TweetS@ was launched to 10,000 ft in the Spaceport America Cup rocketry competition[5] and survived the 100 m/s^2 acceleration, vibrations and a controlled recovery with negligible damage.

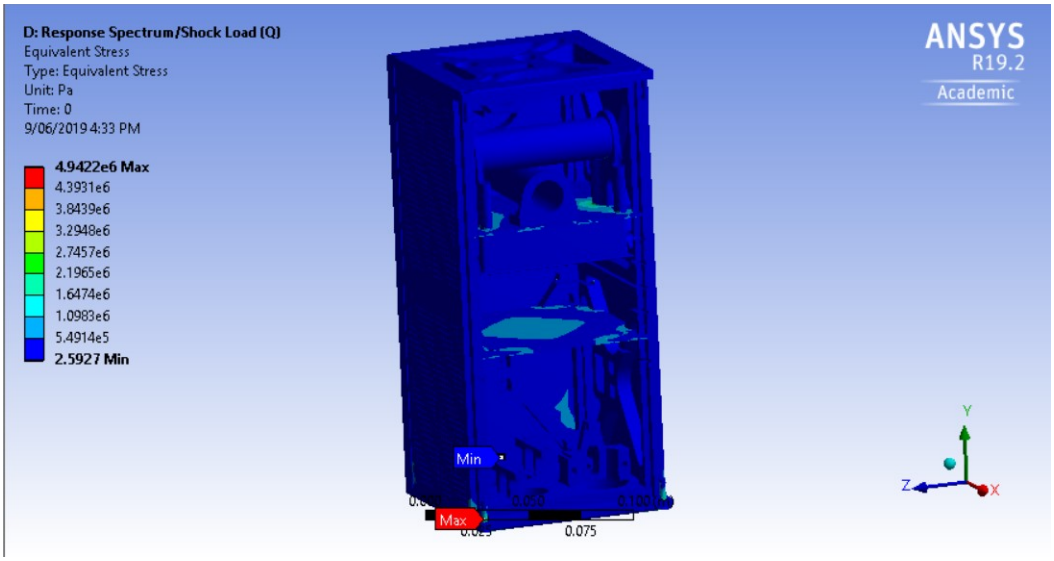

Fig.5: The qualification shock load test performed with a loading of 20 g.

Thermal Results and Analysis

TweetS@ was designed to withstand extreme environmental temperatures in LEO. In space, radiation and conduction constitute the principle forms of heat transfer. The radiation component was further segmented into the three forms: direct solar absorption, albedo (sunlight reflected from the Earth to the spacecraft) and Earth emitted IR (sunlight absorbed by Earth and remitted back out at a different wavelength).

As a benchmark system requirement, controls were designed to withstand hypothetical vacuum chamber cycling and bake out tests based on the extreme operational limits of the most thermally sensitive component of the spacecraft, the battery (-20–50 ˚C). The temperature rate of the cycling test was 2 ˚C per minute for a duration of three hours.

Only passive controls were considered in the form of multi-layered insulation. Mylar was selected as the insulating material due to its low cost and high reflectivity[6] of 95% and because of previous studies of its use in spacecraft [4]. Thermal control validation was conducted via ANSYS transient (time-varying) simulations on a simplified CAD model of the satellite generated in SolidWorks. Three primary scenarios were investigated: one imitating the thermal LEO environment, and the other two simulating the physical thermal cycling and bake out.

[5] sydney.edu.au/news-opinion/news/2019/06/30/sydney-rocketry-team-wins-at-spaceport-america-cup.html

[6] https://www.hydroexperts.com.au/Mylar-Reflective-Film-Roll-1.22M-X-15M-Thickness-1MIL-25. 4um-Highly-Reflective

Since the altitude of LEO orbit placed the satellite in the thermosphere, the ambient environment temperature varied widely depending on which surfaces were exposed to the sun. All radiation processes were conducted in ANSYS using a constant ambient temperature of 20 °C with a smallest mesh size restricted to 2 mm. Furthermore, to ensure power requirements of the CubeSat were met, heat flux absorption values were calculated based on a reference local time of ascending node (LTAN) of 0800 hours, a worst-case scenario with regards to thermal systems.

To obtain heat flux, IR and albedo values for orbital analysis, numerical MATLAB simulations were conducted using the data gathered by the 1980s NASA Earth Radiation Budget Experiment. The longitude and latitude of the satellite's nadir point was calculated using trigonometry to account for the local albedo and IR flux values.

Simulations found that using just one layer of insulation across all tests was enough to keep the battery temperature within operational limits. While other areas of the spacecraft reached temperatures in excess of 100 °C, these were within the operating temperatures of the given components. The camera lens was exposed to capture images; however, its maximum temperature was found to be 75–80 °C which was within its 85 °C limit.

SolarNet

Motivation

The final novel feature implemented on TweetS@ was SolarNet, a machine learning algorithm to determine the sun vector relative to the satellite. This section outlines the motivations behind calculating the sun vector.

There were four measurements available to determine the attitude: the acceleration, the magnetic field and angular rotation from the inertial measurement unit (IMU), and the direction of the sun based off measurements from the solar panels and photodiodes on the external faces of the satellite. The accelerometer was not used because an orbiting object has no relative acceleration. The magnetometer could be used to measure the Earth's magnetic field for an absolute orientation indication based on the satellite location from the GPS. However, the Earth's magnetic field is not easily modelled, and it drifts over time [5]. We were not willing to reserve nor upload on a regular basis to the satellite the large amount of memory required to store the Earth's magnetic field, hence we decided that using the magnetometer for attitude determination was not viable. The final measurement available from the IMU was the gyroscope. The angular rate was accurate and reliable, however it only gave relative changes in attitude, so a form of absolute measurement was required to give the gyroscope readings meaning. The remaining measurement was the sun vector. Its reference vector was easily modellable using a set of rotational transformations from the GPS data, however this measurement was not available during eclipse.

We followed existing literature by using an extended Kalman filter (EKF) with primary dependence on the gyroscope measurements and secondary dependence on sun vector measurements [6]–[8]. The simulated attitude determination results using the EKF (in the form of the cosine similarity between the true and estimated quaternions) is shown in
Figure 6. Cosine similarity between two *n*-dimensional vectors **A** and **B** is defined as

$$\cos(\theta) = \frac{\mathbf{A} \cdot \mathbf{B}}{|\mathbf{A}||\mathbf{B}|}$$

and since each quaternion has a norm of unity, a similarity of 1 indicates **A** = **B**. Without knowledge of the sun vector, the angular rate of the satellite was determinable by the gyroscope, but the quaternions were not. With the inclusion of the sun vector measurements accurate to

only ±30°, the estimated state converged to the true quaternions in less than two minutes—a very small timeframe compared to the overall operation of the satellite.

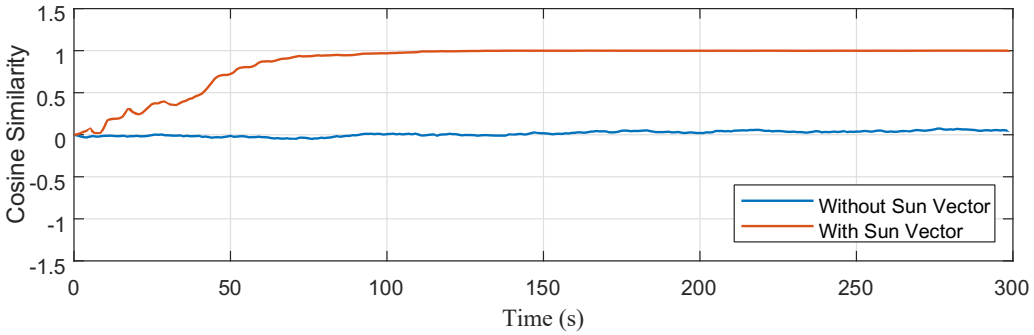

Fig.6: Cosine similarity between the true and estimated quaternions during the EKF simulation with and without the sun vector measurements.

SolarNet was developed as a proof of concept to determine the sun vector from a machine learning perspective. This approach had a large number of advantages over conventional methods of sun vector determination. For example, off-the-shelf CubeSat sun sensors cost thousands of dollars and have a limited field of view[7]. While SolarNet was less precise than these sub-degree accurate sun sensors [9], it only required the addition of four small, low cost current sensors on each of the solar panel power buses and additional photodiode circuits on the end faces. This made it low cost, effective and gave it a full spherical field of view. Other approaches with similar low-cost sensor requirements had been proposed using trigonometric proportions of the face current [10] or narrow field of view photodiodes [11], but these struggle to account for supplementary indecent light from, for example, albedo reflection. Our machine learning approach could be retrained in orbit to account for this. A one-off external determination of the absolute attitude of the satellite (from the camera payload for instance) could be used to initialise the training data collection in orbit. Readings could then be continuously accumulated while the drift of the gyroscope remained negligible.

Architecture and Design

The inputs to SolarNet were the four solar panel current readings and two photodiode voltage measurements. To predict the sun vector, a neural network was used as a function approximator from the six inputs to three outputs. The inputs were first normalised to have zero mean and unit variance.

The model consisted of two densely connected intermediate layers with 12 neurons and a rectified linear unit (RELU) function [12]

$$\mathrm{RELU}(x) = \max(0, x)$$

as the nonlinearity. A visual depiction of the SolarNet architecture is shown in Figure 7.

[7] https://www.cubesatshop.com/product/nss-cubesat-sun-sensor/

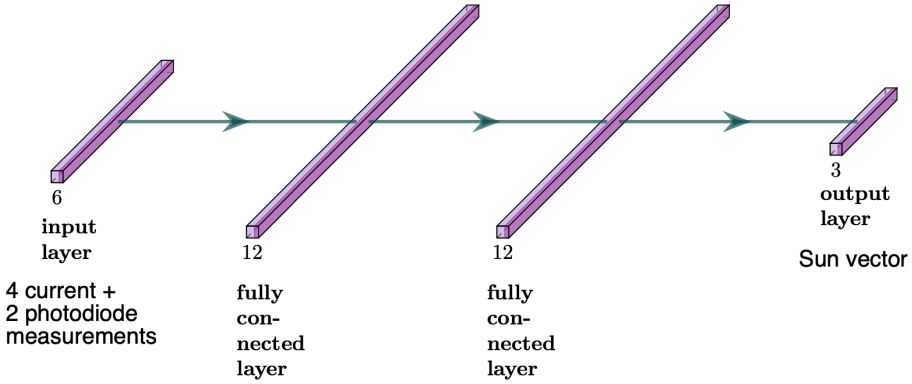

Fig.7: The Multilayer Perceptron SolarNet Architecture

Since the data was collected along a set of manoeuvres, the last 10% of the 1000 collected data points were split into a validation set. The batch size was 128 and Adam optimisation was used during backpropagation to speed up convergence [13].

The output was a unit vector with components varying between ±1. Therefore, the final layer activation function was a tanh function which maps the real numbers onto the interval between ±1. Since the gradients of the tanh function around the ±1 limits are small, it was difficult to train the model to predict these extremes. Therefore, the tanh function was scaled by two, and clipped to force the output between ±1.

The weights for each layer were initialised using Xavier uniform initialisation which drew random numbers from a distribution with zero mean, and variance which depended on the number of connections to each successive layer [14]. This was demonstrated to decrease the effect of vanishing and exploding gradients during backpropagation.

The loss function used was the L1 distance between the predicted value and the true value. Training on a single GPU with a learning rate of 0.003, the model converged in 24 seconds after 1400 gradient steps.

Results and Discussion

Using this architecture on 1000 data points, an accuracy of $\pm 10^{\circ}$ was achieved. While this falls short of commercial CubeSat sun sensors which typically have an accuracy of $\pm 1^{\circ}$ [15], it suffices as a proof of concept. Despite the noise in the data, filtering the input current did not improve the results and led to marginally slower convergence as seen in Figure 8b. This was because the noise had a regularising effect [16].

Performance could have been improved by improving the method of data collection. The training data was collected manually by aligning the base vector of the CubeSat with a spotlight, and then turning it on a music stand and using the gyroscope to collect relative orientation vectors from the initial position. Over the short trajectories collected, the gyroscope's drift was negligible. We estimated the alignment had an accuracy of $\pm 5^{\circ}$, which meant a learnt accuracy of $\pm 10^{\circ}$ was satisfactory. Additionally, the total data collected was insufficient. We collected only 1,000 samples, which fell short of the data typically required to train neural networks for real world applications [17]. Furthermore, a face of the satellite was occasionally obscured by the music stand or our hands during the data collection. Improvements to this process therefore could include using a laser to ensure perfect alignment and gathering more data.

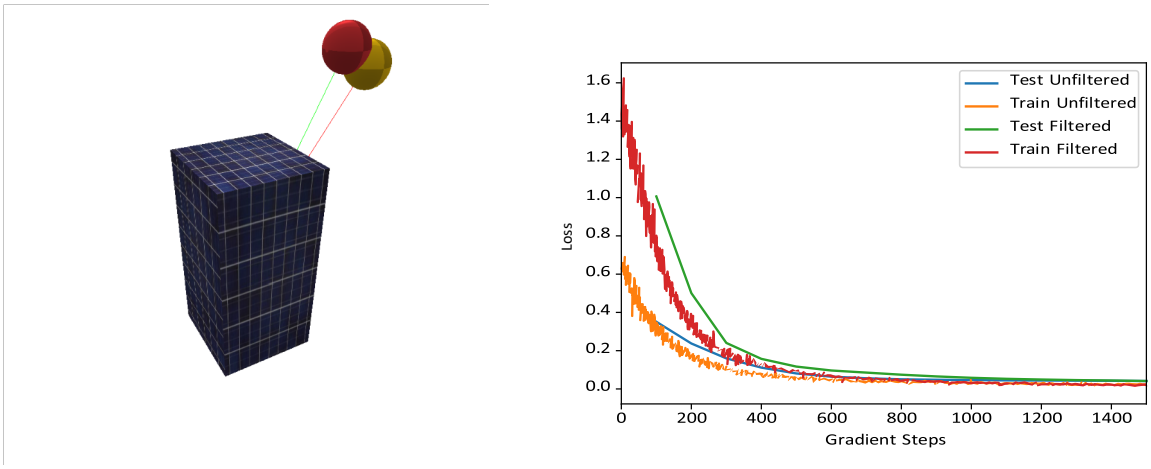

(a) Visualisation of our real data collection, with predicted sun vector (red), vs true sun vector (gold).

(b) Training curves demonstrating equivalent performance when input data was smoothed using a third order lowpass Butterworth filter

Fig.8: Visualisation and performance of SolarNet algorithm

Conclusion

TweetS@ was a project that demonstrated a means for the public to be actively involved with space technology. The final product was a ground-based model of the satellite which integrated with Twitter to increase community engagement in space. The 3D printed structure of this satellite was validated through vibration and thermal simulation tests as well as a physical launch to 10,000 ft. Additionally, this prototype displayed the use of a space and cost-effective machine learning approach for determining the sun vector using solar panel current and photodiode measurements.

Acknowledgements

This work was made possible by the support and advice of Xiaofeng Wu and Iver Cairns at the University of Sydney. We also acknowledge the USYD Rocketry Team for testing TweetS@'s structural capability in the Spaceport America Cup 2019 rocketry competition.

References

[1] J. Clement. (Aug. 2019). Number of monthly active twitter users worldwide from 1st quarter 2010 to 1st quarter 2019 (in millions), [Online]. Available: https://www.statista.com/statistics/282087/number-of-monthly-active-twitterusers/.

[2] J. Jasperneite, M. Schumacher, and K. Weber, "Limits of increasing the performance of industrial ethernet protocols," in *2007 IEEE Conference on Emerging Technologies and Factory Automation (EFTA 2007)*, IEEE, 2007, pp. 17–24.

[3] P. Candini, S. Piattoni, and F. Piergentili, "Plastic cubesat: An innovative and low-cost way to perform applied space research and hands-on education," *Acta Astronautica*, vol. 81, no. 2, pp. 419–429, 2012.

[4] L. Stimpson and W. Jaworski, "Effects of overlaps, stitches, and patches on multilayer insulation.," 1972. [Online]. Available: https://ntrs.nasa.gov/search.jsp?R=19720047163.

[5] R. T. Merrill, M. McElhinny, and P. L. McFadden, *The magnetic field of the earth: Paleomagnetism, the core, and the deep mantle*, ser. International geophysics series.

Academic Press, 1998, isbn: 9780124912465. [Online]. Available: https://books.google.com.au/books?id=96APl4nK9lIC.

[6] D. Choukroun, Y. Oshman, J. Thienel, and M. Idan, *Advances in Estimation, Navigation, and Spacecraft Control: Selected Papers of the Itzhack Y. Bar-Itzhack Memorial Symposium on Estimation, Navigation, and Spacecraft Control*. Springer, 2015, pp. 413–437.

[7] M. L. Psiaki, "Attitude-determination filtering via extended quaternion estimation," *Journal of Guidance, Control, and Dynamics*, vol. 23, no. 2, pp. 206–214, 2000.

[8] F. L. Markley and D. Mortari, "Quaternion attitude estimation using vector observations," *The Journal of the Astronautical Sciences*, vol. 48, no. 2-3, pp. 359–380, 2000.

[9] "Multi-aperture cmos sun sensor for microsatellite attitude determination," *International Journal of Aerospace Engineering Volume 2013, Article ID 549080, 9 pages*, no. 9, pp. 4503–4524, 2009.

[10] R. L. Rocha. R, "Photovoltaic panels as attitude sensors for artificial satellites," *IEEE Aerospace and Electronic Systems Magazine*, 2016.

[11] J. L. Mark A. Post and R. Lee, "A low-cost photodiode sun sensor for cubesat and planetary microrover," *International Journal of Aerospace Engineering*, 2013.

[12] V. Nair and G. E. Hinton, "Rectified Linear Units Improve Restricted Boltzmann Machines," in *27th International Conference on Machine Learning*, 2010. [Online]. Available: https://www.cs.toronto.edu/~fritz/absps/reluICML.pdf.

[13] D. P. Kingma and J. Lei Ba, "ADAM: A Method for Stochastic Optimization," in *International Conference on Learning Representations (ICLR)*, 2015. [Online]. Available: https://arxiv.org/pdf/1412.6980.pdf.

[14] X. Glorot and Y. Bengio, "Understanding the difficulty of training deep feedforward neural networks," in *Proceedings of the thirteenth international conference on artificial intelligence and statistics*, 2010, pp. 249–256.

[15] M. A. Post, J. Li, and R. Lee, "A low-cost photodiode sun sensor for cubesat and planetary microrover," *International Journal of Aerospace Engineering Volume 2013, Article ID 549080, 9 pages*, 2013.

[16] H. Noh, T. You, J. Mun, and B. Han, "Regularizing Deep Neural Networks by Noise: Its Interpretation and Optimization," in *Neural Information Processing Systems, (NIPS 2017)*, 2017. [Online]. Available: https://papers.nips.cc/paper/7096regularizing-deep-neural-networks-by-noise-its-interpretation-andoptimization.pdf.

[17] J. Tobin, R. Fong, A. Ray, J. Schneider, W. Zaremba, and P. Abbeel, "Domain Randomization for Transferring Deep Neural Networks from Simulation to the Real World," in *International Conference on Intelligent Robots and Systems*, 2017.